Original Article

DOI: 10.3348/kjr.2011.12.4.431
pISSN 1229-6929 · eISSN 2005-8330
Korean J Radiol 2011;12(4):431-438

Korean Journal of Radiology
KJR

Segmental Difference of the Hepatic Fibrosis from Chronic Viral Hepatitis due to Hepatitis B versus C Virus Infection: Comparison Using Dual Contrast Material-Enhanced MRI

Jae Ho Shim, MD, Jeong-Sik Yu, MD, Jae-Joon Chung, MD, Joo Hee Kim, MD, Ki Whang Kim, MD

All authors: Department of Radiology and the Research Institute of Radiological Science, Yonsei University College of Medicine, Gangnam Severance Hospital, Seoul 135-720, Korea

Objective: We wanted to identify the geographic differences in hepatic fibrosis and their associations with the atrophy-hypertrophy complex in patients with chronic viral hepatitis using the dual-contrast material-enhanced MRI (DC-MRI) with gadopentetate dimeglumine and ferucarbotran.

Materials and Methods: Patients with chronic C (n = 22) and B-viral hepatitis (n = 35) were enrolled for determining the subjective grade of fibrosis (the extent and thickness of fibrotic reticulations) in the right lobe (RL), the caudate lobe (CL), the medial segment (MS) and the lateral segment (LS) of the liver, with using a 5-grade scale, on the gradient echo T2*-weighted images of DC-MRI. The fibrosis grades of different segments were compared using the Kruskal-Wallis test followed by post-hoc analysis to establish the segment-by-segment differences. The incidences of two pre-established morphologic signs of cirrhosis were also compared with each other between the two groups of patients.

Results: There were significant intersegmental differences in fibrosis grades of the C-viral group (p = 0.005), and the CL showed lower fibrosis grades as compared with the grades of the RL and MS, whereas all lobes were similarly affected in the B-viral group (p = 0.221). The presence of a right posterior hepatic notch was significantly higher in the patients with intersegmental differences of fibrosis between the RL and the CL (19 out of 25, 76%) than those without such differences (6 out of 32, 19%) (p < 0.001). An expanded gallbladder fossa showed no significant relationship (p = 0.327) with the segmental difference of the fibrosis grades between the LS and the MS.

Conclusion: The relative lack of fibrosis in the CL with more advanced fibrosis in the RL can be a distinguishing feature to differentiate chronic C-viral hepatitis from chronic B-viral hepatitis and this is closely related to the presence of a right posterior hepatic notch.

Index terms: *Liver cirrhosis; Magnetic resonance imaging; Gadolinium; Iron; Chronic hepatitis B; Chronic hepatitis C*

Received December 28, 2010; accepted after revision March 2, 2011.

Corresponding author: Jeong-Sik Yu, MD, Department of Radiology, Yonsei University College of Medicine, Gangnam Severance Hospital, 712 Eonjuro, Gangnam-Gu, Seoul 135-720, Korea.
• Tel: (822) 2019-3510 • Fax: (822) 3462-5472
• E-mail: yjsrad97@yuhs.ac

INTRODUCTION

Chronic viral hepatitis is a common cause of hepatic fibrosis and this results in cirrhosis complicated with hepatocellular insufficiency, portal hypertension and an increased risk of hepatocellular carcinoma (1). During the generation of hepatic fibrosis, atrophy of the right lobe (RL) and medial segment (MS), and hypertrophy of the caudate lobe (CL) and lateral segment (LS) could induce expansion of the gallbladder fossa or formation of a right posterior hepatic notch (2). Even though this atrophy-hypertrophy

complex has been used to explain the early morphologic changes of the liver related to the geographic differences of portal venous perfusion or hepatic venous drainage, most of the reports on this were based on observations of the patients in the United States or Japan (3, 4), where the alcoholic hepatitis or chronic hepatitis C virus infection predominates. Yet in clinical practice in our country, this atrophy-hypertrophy complex is not so frequently observed and especially in the cirrhotic patients with chronic hepatitis B viral infection. Because hepatitis B virus is usually associated with macronodular cirrhosis and hepatitis C virus is usually associated with micronodular cirrhosis (5, 6), we hypothesized that the distribution of hepatic fibrosis would differ depending on the type of viral infection, and this might be related to the recently reported differing prevalence of the fibrosis-induced gross morphologic signs between the two types of viral infection (7).

Dual-contrast material-enhanced MRI (DC-MRI) is primarily applied for the assessment of focal lesions, but it also allows for gross inspection of the reticular fibrosis in the background liver (8). Gadolinium chelates display a gradual distribution into fibrotic tissue, thereby causing delayed enhancement of the hepatic septal fibrosis during T1-weighted imaging. Superparamagnetic iron oxides (SPIOs) accumulate within the reticuloendothelial cells of the liver, causing T2 and T2* shortening, and this decreases the signal intensity of the background parenchyma and the regenerating nodules in the cirrhotic liver. Based on a gradient-echo T1-weighted sequence with a longer echo time for T2*-weighted imaging, it was possible to assess the grades of hepatic fibrosis with accuracy comparable to that of histopathologic analysis (8). Therefore, we also hypothesized that direct visualization of reticular fibrosis would enable us to evaluate the geographic differences of the fibrotic changes and their associations with the atrophy-hypertrophy complex of different lobes and segments in cirrhotic livers.

Although this study is primarily for academic interest rather than having a direct clinical impact for patients' care, the purpose of this study was to identify the geographic differences in hepatic fibrosis arising from chronic B or C virus-induced hepatitis and their associations with the morphologic changes of the atrophy-hypertrophy complex with the use of DC-MRI.

MATERIALS AND METHODS

Patients

This retrospective study was approved by our institutional review board, and the requirement for informed consent of the individual patients was waived. By surveying an electronic database of the patients' records from August 2005 to December 2007, we identified 24 patients with chronic hepatitis C virus infection (the C-viral group) who underwent DC-MRI with gadopentetate dimeglumine-enhanced dynamic imaging and ferucarbotran-enhanced delayed phase imaging (8) in the same session at our institution for further examination of suspected hepatic lesions seen by other imaging modalities. We enrolled a total of 22 C-viral group patients (M:F = 17:5; age range, 54-81 years; mean age, 65.5 years). Two patients had been previously treated by transcatheter arterial chemoembolization (TACE) (n = 1) or hepatic resection (n = 1) and they were excluded because these treatments could affect the evaluation of hepatic fibrosis on MR images. We also enrolled 35 consecutive patients during a 6-month period from July 2007 to December 2007 with chronic hepatitis B virus infection (the B-viral group, M:F = 26:9; age range, 40-70 years; mean age, 53.8 years) who underwent the same protocol during the same period. Viral infection was diagnosed by a viral antigen test and by antibody titration, and all patients had a 10-year or longer history of chronic hepatitis. At the time of MRI, the Child-Pugh classification of each group of patients was as follows: the C-viral group (class A: n = 14, class B: n = 2, class C: n = 3, no available data: n = 3) and the B-viral group (class A: n = 24, class B: n = 8, class C: n = 3).

MR Imaging Techniques

MR imaging was performed with a 3 Tesla (T) unit (Signa EXCITE; GE Medical Systems, Milwaukee, WI) for 13 C-viral group patients or with a 1.5T unit (Magnetom Avanto; Siemens, Erlangen, Germany) for all B-viral group patients and nine C-viral group patients. Dynamic contrast-enhanced imaging was obtained using a 3D gradient echo (GRE) sequence with ultrafast image reconstruction in the axial plane by employing parallel imaging algorithms. The 1.5T unit was used under the following conditions: VIBE (volumetric interpolated breath-hold examination), GRAPPA (generalized autocalibrating partially parallel acquisition) factor: 2, repetition time (TR): 4.4 ms, echo time (TE): 2.1 m, flip angle: 10°, matrix: 448 × 224, field of view (FOV): 271

Korean Journal of Radiology
KJR

× 379 mm, slice thickness: 5 mm, slice spacing, 2.5 mm and slices: 72. The 3T unit was used under these conditions: LAVA (liver acquisition with volume acceleration), ASSET (array spatial sensitivity encoding technique) factor: 2, TR/TE: 3.5-4.2/1.0-1.2 msec, flip angle: 10°, matrix: 320 × 256, slice thickness: 5 mm, slice spacing: 2.5 mm, slices and 64 depending on the MRI vendor. A dynamic series consisted of one precontrast series followed by three postcontrast series, including the arterial, portal and five-minute delayed phase imaging. The postcontrast series was performed after administering a bolus injection of 0.1 mmol/kg gadopentetate dimeglumine (Magnevist; Bayer HealthCare Pharmaceuticals Inc., Wayne, NJ) at a rate of 2 mL/sec followed by a saline flush using a power injector.

After the dynamic imaging, ferucarbotran (8 μmol iron/kg of Resovist; Bayer HealthCare Pharmaceuticals Inc.) was intravenously administered as the second contrast agent of SPIO. After 10 minutes, the T2-weighted fast spin-echo and T1-weighted double echo chemical shift gradient-echo images were obtained using the same parameters as for the pre-contrast imaging. A gradient-echo sequence with a longer echo time (TR/TE: 134/10 msec, flip angle: 35° or TR/TE: 196/10 msec, flip angle: 30° depending on the MRI vendor) was added for the post-SPIO T2*-weighted imaging. All scans were sent to our picture archiving and communication system (PACS) for interpretation on PACS workstations.

Image Evaluation

Two independent radiologists with 15 and one years of experience, respectively, in hepatic MRI retrospectively reviewed the images in a random order on four side-by-side picture archiving and communicating system monitors, where each gray-scale image was at a 2048 × 2560-pixel resolution (Totoku, Tokyo, Japan). The reviewers were blinded to the demographic, clinical, laboratory and pathology data at the time of the image review. For grading the fibrosis, the liver was divided into 4 segments: RL, CL, MS and LS. Based on the DC-MRI depiction of hepatic fibrosis as proposed by Aguirre et al. (8), the fibrosis grade of each hepatic segment was subjectively assessed using a 5-grade scale from 0: reticulations are not visible on any section to 4: diffuse reticulations are obvious in the entire segment on the post-SPIO T2*-weighted gradient-echo images.

To evaluate the association between the previously-defined morphologic signs of cirrhosis and the presence of geographical differences of reticular fibrosis, the intersegmental differences of the fibrosis grade of MS versus LS, and RL versus CL were compared with the presence of the expanded gallbladder fossa sign and the right posterior hepatic notch sign, respectively (3, 4). The expanded gallbladder fossa sign was considered present if the gallbladder was bound medially by the edge of the lateral segment of the left hepatic lobe below the lowermost portion of the medial segment (3), and the right posterior notch sign was considered to be present when there was a sharp indentation in the right medial posterior surface of the liver (4). The intersegmental difference in hepatic fibrosis was defined as differences of one or more fibrotic grades between the relevant hepatic segments. The portal phase images of a 3D dynamic series (2.5 mm section thickness) were used to determine the presence or absence of the two morphological signs. To minimize discrepancy in the subjective grading of hepatic fibrosis and the presence of morphological signs between the two observers, a consensus was reached for further analyses in all cases after the calculating the interobserver variation.

Statistical Analysis

Interobserver agreement was assessed with the linear weighted kappa statistics for the fibrotic grade or the kappa statistics for the presence of morphological signs, respectively. The level of agreement was defined as follows: a kappa value of 0.2 or less indicated poor agreement, 0.2-0.4 indicated fair agreement, 0.4-0.6 indicated moderate agreement, 0.6-0.8 indicated good agreement and 0.8-1.0 indicated excellent agreement.

The Child-Pugh class of each group of patients were compared with each other using Chi-square tests. The Mann-Whitney test was used to assess the difference of the overall fibrotic severity between the C-viral and B-viral groups. For each chronic hepatitis group, the fibrosis grades of different segments were compared using the Kruskal-Wallis test followed by post-hoc analysis (Tukey's test) to establish the segment-by-segment differences. Pearson's chi-square test or Fisher's exact test was used to assess the relationship between the presence of morphological signs and the intersegmental differences (1 or a larger score in each patient) of the hepatic fibrosis. A p value of less than 0.05 was considered significant. The statistical analysis was done using Sigmaplot, version 10.0 for Windows.

RESULTS

The weighted kappa values for the assessment of the fibrosis grading and the morphologic signs of cirrhosis were 0.61 and 0.65, respectively. This means that the interobserver agreements were good for both analyzed items. The results of the fibrotic grades and their comparisons between the C-viral and B-viral groups are shown in Table 1. The mean value of the fibrotic grade of the RL was highest, followed by that in the MS, LS and CL in the C-viral group. For the Child-Pugh classification, there was no remarkable difference between each of the viral groups (p = 0.914). There were significant differences of the fibrosis grades of each of the hepatic segments in the C-viral group (p = 0.005), and by multiple pairwise comparisons using Tukey's test, the CL showed a significantly lower degree of fibrosis compared to that of the RL and MS, while there were no significant intersegmental differences for the RL, MS and LS (p > 0.05) (Figs. 1, 2). There was a marginal difference of fibrosis between the CL and LS in the C-viral group (p = 0.048). In the B-viral group, there was no statistically significant difference in the fibrosis grade among the different segments (p = 0.221) (Fig. 3).

Among the 57 patients, all eight patients with more advanced fibrosis of the MS, as compared to the LS, had signs of an expanded gallbladder fossa (100%), whereas 40 (82%) of the remaining 49 patients with homogeneous fibrosis had the same signs (p = 0.327) (Table 2). The signs of a right posterior hepatic notch were significantly higher in the patients with intersegmental differences of fibrosis (19 out of 25, 76%) between the RL and CL as compared to that of the other patients (6 out of 32, 19%) (p < 0.001) (Table 2).

Table 1. MRI Fibrosis Grades of C-Viral and B-Viral Groups (57 Patients)

Fibrosis Grading	C-Viral Group (n = 22)	B-Viral Group (n = 35)
Caudate lobe	1.86 ± 1.08	2.36 ± 1.10
Right lobe	2.91 ± 1.06	2.77 ± 0.94
Medial segment	2.77 ± 0.97	2.70 ± 0.94
Lateral segment	2.48 ± 0.96	2.40 ± 1.07
P value	0.005	0.221

Note.— Data are mean ± standard deviation. *P* values are for difference between results from C-viral group and B-viral group.

DISCUSSION

To date, a number of methods have been proposed for the non-invasive identification of hepatic fibrosis; these include serum marker panels and conventional imaging techniques such as ultrasonography, CT and conventional MRI based on the morphological consequences of fibrosis and the stigmata of portal hypertension (2-4, 9-12). The advanced imaging technologies have recently enabled non-invasive tests that reflect the full spectrum of hepatic fibrosis and cirrhosis and its severity in liver diseases (8, 13, 14). One of them is DC-MRI as suggested by Aguirre et al. (8), and

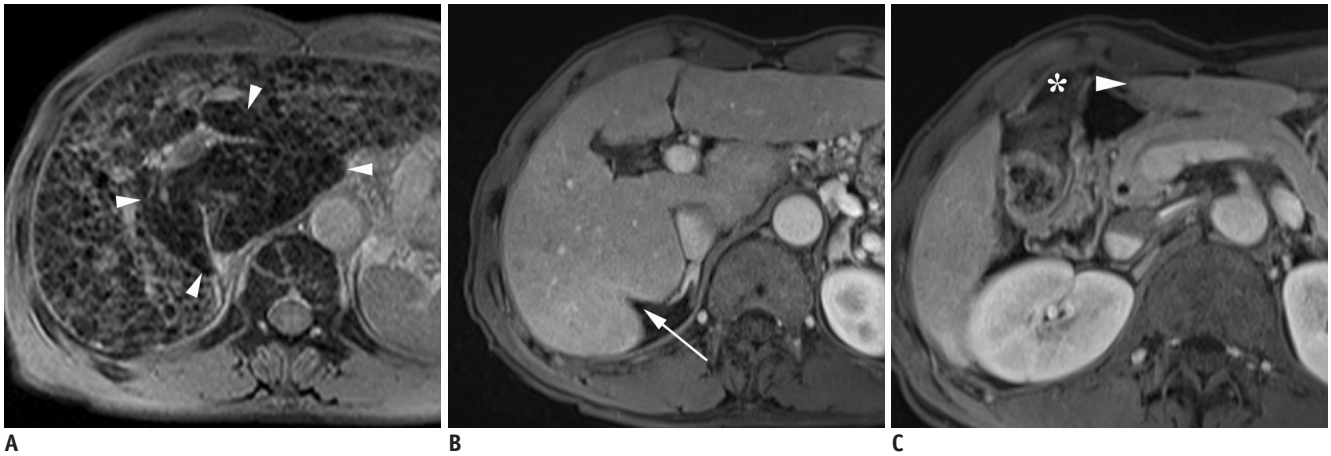

Fig. 1. 60-year-old man with C-viral induced cirrhosis.
A. Double contrast material-enhanced gradient echo (196/10 msec) T2*-weighted image obtained by 1.5T unit depicts diffuse hyperintense reticulations in entire liver except area of hypertrophic caudate lobe (arrowheads). **B.** On transverse 3D gradient echo MR images (4.4/2.1 msec) below level of **A**, right posterior hepatic notch (arrow) is seen between right lobe and caudate lobe. **C.** Transverse 3D gradient echo MR image (4.4/2.1 msec) demonstrates medial portion of lateral segment (arrowhead) is separated from gallbladder (asterisk) without intervening with medial segment, and this represents expanded gallbladder fossa sign below level of **B**.

Korean Journal of Radiology
KJR

A B

Fig. 2. 61-year-old man with C-viral induced cirrhosis.
A. Double contrast material-enhanced gradient echo (140/5.8 msec) images obtained by 3T unit depict diffuse involvement of reticular fibrosis involving entire liver except for small portion of caudate lobe (arrowheads). **B.** There is no hypertrophy of caudate lobe and 3D gradient echo (4.0/1.0 msec) image shows smooth curvature of right posterior medial margin of liver (arrowheads) without any notch formation.

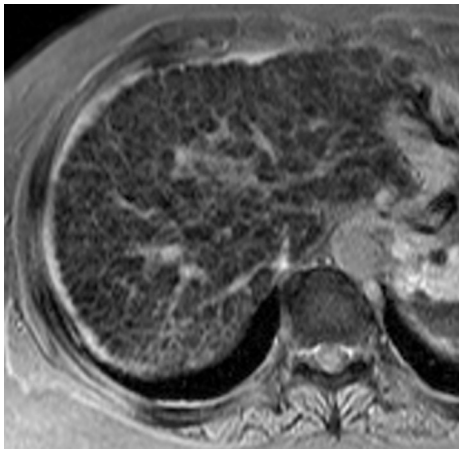

Fig. 3. 60-year-old woman with B-viral induced cirrhosis.
Double contrast material-enhanced gradient echo (196/10 msec) T2*-weighted hepatic MR image obtained by using 1.5T unit depicts homogeneous reticular fibrosis involving entire liver without any evidence of caudate lobe hypertrophy.

Table 2. Correlation between Intersegmental Differences of Fibrotic Grades and Two Morphologic Signs of Hepatic Fibrosis in 57 Patients with Chronic Viral Hepatitis

MS versus LS†	Expanded Gallbladder Fossa Sign	
	+	-
+	8 (14%)	0
-	40 (70%)	9 (16%)
P value	0.327	
RL versus CL‡	Right Posterior Hepatic Notch Sign	
	+	-
+	19 (33%)	6 (11%)
-	6 (11%)	26 (46%)
P value	< 0.001	

Note.— Numbers are number of patients. †Intersegmental difference (≥ 1 in each patient) of fibrosis grade between medial and lateral segments of left lobe, ‡Intersegmental difference (≥ 1 in each patient) of fibrosis grade between right lobe and caudate lobe. + = present, - = not present, CL = caudate lobe, LS = lateral segment of left hepatic lobe, MS = medial segment of left hepatic lobe, RL = right lobe

by using this method, one could achieve direct visualization of the reticular fibrosis and regenerating nodules, as well as an accuracy of greater than 90% for diagnosing the grade of fibrosis, which is an accuracy comparable to that achieved using histopathology analysis. In the latest study of ours (7), we found a close relationship between the prevalence of gross morphologic signs and the degree of hepatic fibrosis in the entire liver as determined on DC-MRI. Moreover, according to the results of our previous study (7), there was a substantial difference in the appearance of gross morphologic signs between the hepatitis B and C viral infections that cause hepatic fibrosis. Depending on the ability to directly visualize the entire liver, DC-MRI can be expected to define the possible geographic or segmental differences of the fibrotic change, which would not be uniform across the entire organ. It can also be presumed

that there would be a relationship between the gross morphologic signs and the segmental distribution of hepatic fibrosis in each of the viral hepatitis groups of patients in the present study.

Using DC-MRI, our results indicate that the CL is significantly spared from fibrosis compared with the RL and MS, and especially in those patients with hepatitis C. Several mechanisms have been suggested to explain the sparing of the CL; these relate to the geographic differences in the portal venous perfusion, which result in volume redistribution in the cirrhotic liver (9, 15). Portal venous blood is essential for liver regeneration because of the various trophic factors in it (16). Because the portal veins in the CL have a shorter intrahepatic course than do the other vessels and because of the proximity veins to the main portal vein, in addition to the short accessory hepatic veins, the portal blood flow and the hepatic venous drainage of the CL might be less affected by fibrotic distortion than the other lobes. The main portal vein splits into the right and left lobar branches at the porta hepatis, and the right portal vein branch enters directly into the parenchyma of the right lobe. Progression of hepatic fibrosis gradually attenuates the intrahepatic portal venous branches and the hepatic venous branches, thereby reducing the hepatic vascular bed (17). Compression of the hepatic venous tributaries by regenerating nodules or fibrosis impairs drainage of blood from the liver, which increases the resistance to portal flow and decreases the right portal blood flow (18). The left lobar branch of the portal vein courses outside the liver parenchyma along the ligamentum venosum before entering into the hepatic parenchyma, resulting in a relatively greater blood supply to the left lobe.

One of the most interesting findings in the present study was the lack of remarkable intersegmental differences in hepatic fibrosis in those patients with hepatitis B. One potential explanation is the different pathological factors between the two groups. Cirrhosis can be divided by the gross pathology into micronodular, macronodular and mixed-forms according to the size of the regenerating nodules. In those patients with hepatitis B, the size of the regenerative nodules is heterogeneous. However, in this patient group there are more macronodules, and the intervening fibrotic septa are thinner than that in the patients with hepatitis C, who tend to have micronodules with thicker septa (19). Nagula et al. (20) demonstrated that small nodularity and thick septa are independent predictors of the presence of clinically significant portal hypertension. Thick septa would induce wide tissue collapse and passive obstruction to the portal venous flow. Small nodules are also indicative of greater damage and greater architectural distortion and the small nodules will further increase intrahepatic resistance (21). We can speculate that during the early stage of hepatic fibrosis, the fibrotic process might be geographically different depending on the inherent segmental differences of the portal venous perfusion pressure. It is well known that compared with the CL, the RL is more peripherally located from the hepatic hilum and the portal venous perfusion pressure is relatively lower. The different perfusion pressure gradients between the CL and RL would increase the portal blood flow to the CL due to the CL's low resistance to portal venous perfusion, while the RL would receive less portal venous perfusion due to the RL's higher resistance. In the patients of the C-viral group, thick septal fibrosis and micronodules will induce more profound regional variations of the portal perfusion within the liver and they will synergistically induce more profound regional variations of the hepatic fibrosis, as compared to that of the hepatitis B patients with macronodules and thin septa. The geographical heterogeneity of hepatic fibrosis observed in our study was grossly correlated with the gross hepatic volume redistribution in the right posterior notch, indicating atrophy-hypertrophy of the RL and CL. As is observed in daily practice, in advanced macronodular cirrhosis, the fibrotic reticulations and regenerative nodules tend to be more evenly distributed within the whole liver, and CL hypertrophy and the appearance of the right posterior hepatic notch are uncommon. For most of the hepatitis B patients with thin fibrotic septa and larger regenerating nodules in our present study, the regional or intersegmental variation in the portal perfusion seems to be too small to cause apparent geographic differences, regardless of the stage of hepatic fibrosis.

Although all eight patients with a higher fibrosis grade in the MS as compared to that in the LS had an expanded gallbladder fossa, we could not find meaningful differences of the incidence of this morphologic sign between these patients and the others due to the overall high prevalence of this sign in the patients without such segmental differences. Initially, we expected that the signs of an expanded gallbladder fossa would appear more frequently in the patients with segmental differences in fibrosis between the LS and the MS, like the condition between the CL and the RL. Besides the limited number of patients

Korean Journal of Radiology
KJR

who showed different fibrotic grades between the LS and the MS, there may be another explanation for the lack of statistical significance. Unlike other hepatic segments, the portal venous perfusion in the MS is easily decreased in the early stage of hepatic fibrosis. This is due to the unique anatomical direction of the portal venous flow observed with using color Doppler ultrasonography (22). The flow in the portal vein branches of the LS and the CL is uniformly hepatopetal, whereas the MS often receives circular or hepatofugal flow from the right side of the umbilical segment with less blood than the other segments (23). Even during early fibrosis, which cannot be grossly depicted on DC-MRI, the overall portal venous perfusion is usually reduced in the entire liver, and the flow to the MS would be more deteriorated and minimized earlier than the flow in the other segments, resulting in segmental atrophy (23). For the high prevalence of expanded gallbladder fossa signs regardless of the intersegmental difference between the MS and the LS in the present study, the expanded gallbladder fossa sign may develop before the gross appearance of reticular fibrosis.

This study has several limitations. Our patients did not have histopathologically confirmed liver cirrhosis; however, meticulous fibrosis grading of each hepatic segment for the explanted livers or multiple biopsy procedures for each segment for this purpose would not be practical. It should be emphasized that we focused on the relative differences of the fibrosis grades among the hepatic segments rather than on the absolute fibrosis grade in each hepatic segment. Second, our study was limited by the small size of the C-viral group compared to that of the B-viral group in our country, and the B-viral patients were randomly selected for comparative analyses. However, there was no difference in the overall fibrotic severity between the C-viral and B-viral groups, and we believe that there were no considerable selection biases that would alter the results of this study. Finally, we know our study was not like previous studies that determined the severity of cirrhosis to support the treatment plan in cirrhotic patients. Our study was motivated by academic interest from the observations in daily practice. Moreover, the differential diagnosis between C-viral and B-viral on DC-MRI would not have a big clinical implication in the practical manner. We just hoped to contribute insight on the hemodynamic changes in the cirrhotic liver depending on the viral type along with a better understanding of the morphological changes of cirrhotic livers.

In conclusion, DC-MRI demonstrated the geographic or intersegmental differences of hepatic fibrosis in the C-viral group as distinguished from those of the B-viral group, and there were no remarkable variations among the different hepatic segments. Our results suggest that the relative lack of fibrosis in the CL and the more advanced fibrosis in the RL causes a right posterior hepatic notch, and especially in the patients with chronic C-viral hepatitis, whereas expansion of the gallbladder fossa is not closely related to the intersegmental differences in hepatic fibrosis regardless of the sorts of the viruses.

REFERENCES

1. Custer B, Sullivan SD, Hazlet TK, Iloeje U, Veenstra DL, Kowdley KV. Global epidemiology of hepatitis B virus. *J Clin Gastroenterol* 2004;38:S158-168
2. Ito K, Mitchell DG. Imaging diagnosis of cirrhosis and chronic hepatitis. *Intervirology* 2004;47:134-143
3. Ito K, Mitchell DG, Gabata T, Hussain SM. Expanded gallbladder fossa: simple MR imaging sign of cirrhosis. *Radiology* 1999;211:723-736
4. Ito K, Mitchell DG, Kim MJ, Awaya H, Koike S, Matsunaga N. Right posterior hepatic notch sign: A simple diagnostic MR finding of cirrhosis. *J Magn Reson Imaging* 2003;18:561-566
5. Okazaki H, Ito K, Fujita T, Koike S, Takano K, Matsunaga N. Discrimination of alcoholic from virus-induced cirrhosis on MR imaging. *AJR Am J Roentgenol* 2001;175:1677-1681
6. Anthony PP, Ishak KG, Nayak NC, Poulsen HE, Scheuer PJ, Sobin LH. The morphology of cirrhosis. Recommendations on definition, nomenclature, and classification by a working group sponsored by the World Health Organization. *J Clin Pathol* 1978;31:395-414
7. Yu JS, Shim JH, Chung JJ, Kim JH, Kim KW. Double contrast-enhanced MRI of viral hepatitis-induced cirrhosis: correlation of gross morphological signs with hepatic fibrosis. *Br J Radiol* 2010;83:212-217
8. Aguirre DA, Behling CA, Alpert E, Hassanein TI, Sirlin CB. Liver fibrosis: noninvasive diagnosis with double contrast material-enhanced MR imaging. *Radiology* 2006;239:425-437
9. Di Lelio A, Cestari C, Lomazzi A, Beretta L. Cirrhosis: diagnosis with sonographic study of the liver surface. *Radiology* 1989;172:389-392
10. Dodd GD 3rd, Baron RL, Oliver JH 3rd, Federle MP. Spectrum of imaging findings of the liver in end-stage cirrhosis: part I, gross morphology and diffuse abnormalities. *AJR Am J Roentgenol* 1999;173:1031-1036
11. Ito K, Mitchell DG, Gabata T. Enlargement of hilar periportal space: a sign of early cirrhosis at MR imaging. *J Magn Reson Imaging* 2000;11:136-140
12. Awaya H, Mitchell DG, Kamishima T, Holland G, Ito K, Matsumoto T. Cirrhosis: modified caudate-right lobe ratio.

Radiology 2002;224:769-774
13. Castéra L, Vergniol J, Foucher J, Le Bail B, Chanteloup E, Haaser M, et al. Prospective comparison of transient elastography, Fibrotest, APRI, and liver biopsy for the assessment of fibrosis in chronic hepatitis C. *Gastroenterology* 2005;128:343-350
14. Huwart L, Sempoux C, Salameh N, Jamart J, Annet L, Sinkus R, et al. Liver fibrosis: noninvasive assessment with MR elastography versus aspartate aminotransferase-to-platelet ratio index. *Radiology* 2007;245:458-466
15. Zhou X, Lu T, Wei Y, Chen X. Liver volume variation in patients with virus-induced cirrhosis: findings on MDCT. *AJR Am J Roentgenol* 2007;189:w153-159
16. Starzl TE, Francavilla A, Halgrimson CG, Francavilla FR, Porter KA, Brown TH, et al. The origin, hormonal nature, and action of hepatotrophic substances in portal venous blood. *Surg Gynecol Obstet* 1973;137:179-199
17. Huet PM, Pomier-Layrargues G, Villeneuve JP, Varin F, Viallet A. Intrahepatic circulation in liver disease. *Semin Liver Dis* 1986;6:277-286
18. Popper H. Pathologic aspects of cirrhosis. A review. *Am J Pathol* 1977;87:228-264
19. Shimamatsu K, Kage M, Nakashima O, Kojiro M. Pathomorphological study of HCV antibody-positive liver cirrhosis. *J Gastroenterol Hepatol* 1994;9:624-630
20. Nagula S, Jain D, Groszmann RJ, Garcia-Tsao G. Histological-hemodynamic correlation in cirrhosis-a histological classification of the severity of cirrhosis. *J Hepatol* 2006;44:111-117
21. Ganne-Carrié N, Ziol M, de Ledinghen V, Douvin C, Marcellin P, Castera L, et al. Accuracy of liver stiffness measurement for the diagnosis of cirrhosis in patients with chronic liver diseases. *Hepatology* 2006;44:1511-1517
22. Rosenthal SJ, Harrison LA, Baxter KG, Wetzel LH, Cox GG, Batnitzky S. Doppler US of helical flow in the portal vein. *Radiographics* 1995;15:1103-1111
23. Lafortune M, Matricardi L, Denys A, Favret M, Dery R, Pomier-Layrargues G. Segment 4 (the quadrate lobe): a barometer of cirrhotic liver disease at US. *Radiology* 1998;206:157-160